Extracting Bridge Components from a Laser Scanning Point Cloud

Truong-Hong, Linh; Lindenbergh, Roderik

Important note
To cite this publication, please use the final published version (if applicable).
Please check the document version above.

Storage Tank Inspection Based Laser Scanning

L. Truong-Hong[1,*], R. Lindenbergh[1] and P. Fisk[2]

[1]*Department of Geoscience and Remote Sensing, Delft University of Technology, The Netherlands*

[2]*Ironhide Inspection Inc., Calgary, Canada*

[*]*Corresponding author: l.truong@tudelft.nl*

Abstract: Development of laser scanning has offered great opportunity to capture three-dimensional (3D) topographic information of objects' surfaces in a highly accurately and efficiently. Particularly, a terrestrial laser scanner is able to acquire millions of points within a second at millimetre accuracy. This technology has been widely used in many civil engineering applications, including surveying, construction management, and infrastructure inspection. Traditionally, tank inspection was carried out on-site by physical inspectors with suitable measurement equipment (e.g. tapes, staffs and a total station). This approach, albeit the most common one, has many downsides: subjective results, slow and expensive procedure, requirement of experienced and trained inspectors and close service of the tank. Additionally, all results are stored as hard copies, which lead to difficulties in tracking damage development and management. To mitigate these disadvantages, this paper proposes a method for (i) automatically extracting a point cloud of a tank wall from a massive data points, and (ii) evaluating the tank wall through its deformation.

Keywords: *Tank Inspection; Deformation; Feature extraction; Laser scanning; Point Cloud*

1   Introduction

Recent development of laser scanning technology allows to capture three-dimensional (3D) topographic data of visible surfaces of objects in details with high accuracy in short time. This has enabled various applications of laser scanning data in civil engineering for example building reconstruction (Truong-Hong et al., 2012), construction management (Bosché et al., 2015), infrastructure monitoring and inspection (Truong-Hong & Laefer, 2015). Particularly, terrestrial laser scanning data associated existing methods have been widely used in identifying damage of structures' surfaces (Laefer et al., 2014). The highly accurate, dense point cloud can be rich information to automatically inspect damage of a tank associated with its components. That can be an alternative solution to replace this current method, which relies on manual measurements, for example using tapes, or on low sampling data from a total station. However, automatic extracting and detecting damage of the tank are still a challenge task because point clouds corresponding to individual components of the tank have to extracted from a massive point clouds of the complex structure including the tank components associated with other facilities. Thus, this paper proposes a RANSAC-based method empowered by voxelization to efficiently extract the point cloud of the tank wall and subsequently assess damage of the tank through its deformation.

2   Related works

The critical issue in automatic determination of deformation of a tank wall is to extract a point cloud of the tank wall from massive data points of a complex structure consisting of the tank wall and its components (e.g. floor, floating roof, roof, columns, girders, so on), objects surrounding the tank and other facilities (e.g. stair, pipes). In practice, the tank walls mostly appear as a vertical cylinder and are subjected to the surface's damage/deformation after a certain service time. Therefore, this section is focused to survey existing methods for extracting the cylinder from the point cloud.

Most of methods for extracting point cloud representing to a cylinder were based on classification or segmentation of raw point clouds to determine descriptive parameters of the cylinder, which can be Random Sample Consensus (RANSAC) based- and Hough Transform (HT) based-methods (Nurunnabi et al., 2019). In among of RANSAC based methods, it can highlight the algorithm developed by Schnabel et al. (2007) widely popular use in extracting the point cloud of the cylinder. The method estimated a direction of the cylinder's axis as a cross-product of normal vectors of data points, while the center and a radius of the cylinder were determined from the best fit circle of the points on the plane perpendicular to the cylinder's direction. One advantage of the proposed method was a sampling strategy allowing to handle a massive data. However, the method was also required users to tune input parameters (e.g. the minimum points of the estimated cylinder - *min_ptc*, the maximum distance from the point to the estimated cylinder - ε_{max}, and a deviation of points' normal vectors to the cylinder's

normal at the points - α) to obtain the best cylinder. Similarly, Tran et al. (2015) proposed an iterative algorithm to estimate the cylinder's parameters from a random points associated with their normal vectors, and for each iteration inlier points were remained for a next iteration.

On another hand, Rabbani and Van Den Heuvel (Rabbani & Van Den Heuvel, 2005) proposed a sequential generalized HT to extract a point cloud of a cylinder. The HT was first applied to a Gaussian image of the normal vectors of the points to estimate the direction of a cylinder's axis and the points within the highest cell for voting the direction were then used in a second step. Second, the points were then projected onto the orthogonal plane of the cylinder's direction and the HT was used to estimate the center and radius of the cylinder from these projected points. Additionally, Figueiredo et al. (2019) improved HT methods for cylinder detection by introducing a new randomized sampling scheme to create non-uniform orientation Hough accumulators and efficient Hough voting scheme allowing to incorporate curvature information of each cell in the orientation Hough accumulators in the voting scheme. The authors addressed the proposed method can reduce space and executing time.

Although both RANSAC-based and HT-based methods were successful in extracting the cylinder from point clouds, these methods are still problematic with a large data set (Maalek et al., 2019), for example the point cloud of a storage tank is up to hundreds of million points, because these methods are quired normal vectors of the input data. Moreover, it is also difficult to tune many input parameters to obtain the best model, particularly for the tank wall subjected to deformation (including global and local deformations). As such, this paper proposed a RANSAC-based voxelization method to extract the tank wall, in which the method does not required to compute normal vectors of all data points.

3   Proposed method

A goal of the proposed method is to automatically extract the point cloud of a tank wall from entire scanning point clouds, which consist of the points of the tank associated with its components (e.g. a floor, floating roof, roof, girders, columns and rafters), other facilities (e.g. stair, pipes), and other objects (e.g. ground objects) surrounding the tank. Subsequently, the tank wall was evaluated through deformation computed from the data points of the tank wall. In practice, the most tank walls appear as a perfectly vertical cylinder, but during service and/or errors from data acquisition the shape of the tank wall may be an inclined and/or imperfect cylinder. In addition, to identify surface damage, the tank was often scanned with a high resolution resulting the point cloud of the tank up to hundreds of million points. To solve these problems, the proposed method involves 4 main steps (Fig. 1) to extract the point cloud of the tank wall. In Step 1, an input point cloud was decomposed into an octree representation and the voxels contain candidate points of the tank wall were extracted based on a deviation angle between the normal vectors of the voxels and a unit vector of the oz axis in Step 2. Subsequently, in Step 3, the RANSAC-based voxelization method was proposed to estimate a fitting cylinder of the tank wall, which can allow to easily to retrieve the points of the tank wall. Finally, Step 4 computes deformation of the tank wall based on its fit cylinder (known as the vertical fit and the best fit cylinders), which is to determine if the tank deformation is exceeded a limitation.
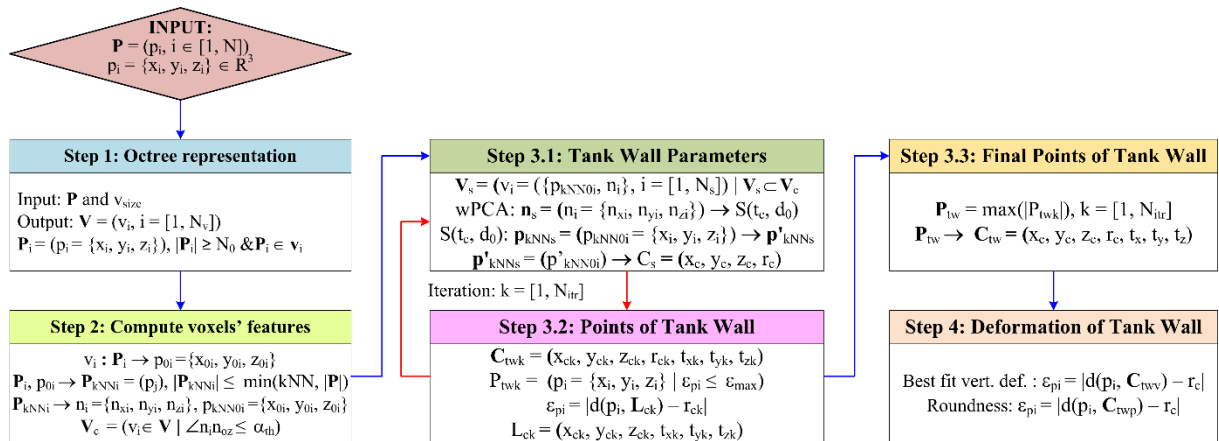

Figure 1. Proposed workflow to determine deformation of the tank wall

In practice, during capturing a storage tank, the point cloud involves not only the tank's components but also other facilities and environmental objects. An input data points, $\mathbf{P} = (p_i = \{x_i, y_i, z_i\} \in R^3, i = [1, N])$ may consist of hundreds of million points. To reduce intensive computation, in Step 1, an octree representation (Fig. 2a) was employed to recursively subdivide an initial enclosing bounding box of an input point cloud P into the smaller

voxels until a terminal condition is reach. In this study, the maximum size of the voxels (v_{size}) on leaf nodes of the octree was used, which is 0.5m, although several other terminal conditions have been used, for example, a maximum depth or the maximum number of points within the voxel. Each voxel is defined as classification, address and geometry. The voxels are classified as "full" if the voxel contains the number of points equal or larger than a predefined threshold, which is empirically selected as 10 points; otherwise, the voxels were classified as "empty". Similar Truong-Hong et al. (Truong-Hong & Laefer, 2014), an address of the voxel is to indicate the relationship between the voxel to its parent voxel and its sibling voxels (Fig. 2a). Moreover, the voxel's geometry is defined as x-, y-, z- coordinates of two opposite corners of the voxel. A subdivision process is only carried out on the full voxels. Fig. 2b & c show the full voxels generated from the point cloud of the exterior tank.
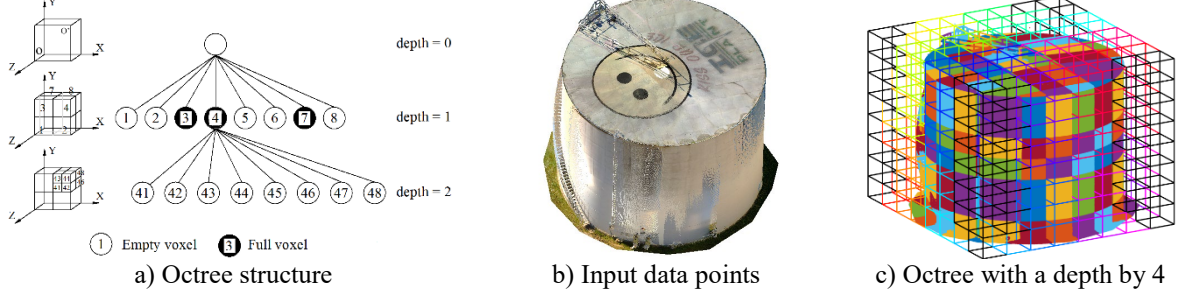

| a) Octree structure | b) Input data points | c) Octree with a depth by 4 |

Figure 2. Octree representation

Next, Step 2 is to compute features of the full voxels on leaf nodes of the octree representation to provide information for estimating parameters of a cylinder of a tank wall. First, a normal vector of each full voxel ($v_i \in$ **V**, i = [1, N_v]) is computed, which was defined as the normal vector of a local planar surface at the center of the points within the voxel. As such, from the voxel center (p_{0i}) computed the points (**P_v**) within the voxel (Eq. 1), the k-nearest number (kNN) of neighbor points (P_{kNN}) is extracted and the normal vector ($n_i = \{n_{xi}, n_{yi}, n_{zi}\}$) of the plane through P_{kNN} is an eigenvector corresponding to the smallest eigenvalue computed from a covariance matrix (Eq. 2) by using a robust principal component analysis rPCA (Laefer & Truong-Hong, 2017). In this study, kNN by 25 points is empirically used. Notably, for searching the neighbor points, only the points within the voxel are used, which implied $|P_{kNN}| \leq |$ **P_v** $|$. Moreover, after estimating the normal vector n_i, the new center of the voxel is also updated based on the kNN points (Eq. 1).

$$p_{0i} = \frac{1}{|P_v|}\sum_{p_j \in P_v} p_j \tag{1}$$

$$C_{kNN} = \frac{\sum_{p_j \in P_{kNN}} w(p_j)(p_j - p_{kNN0i})(p_j - p_{kNN0i})^t}{\sum_{p_i \in P_{kNN}} w(p_i)} \tag{2}$$

$$w(p_j) = exp(\frac{-d_{pj}^2}{d_0^2}) \tag{3}$$

where p_{0i} is a center of the voxel v_i computed from the **P_v**, $|$ $|$ is the cardinal of the P_v, C_{kNN} is a covariance matrix computed from P_{kNN}, in which p_{kNN0i} is the centroid of the P_{kNN} computed from Equation 1, $w(p_j)$ is the weight of each point $p_j \in$ **P_{kNN}**, d_{pj} is the distance between point p_j to a plane through P_{kNN}, and d_0 is set equal to $1/5\Sigma d_{pj}$.

By observing the tank configuration, the tank wall is mostly vertical, which is implied if a voxel contains the points of the tank wall, its normal vector is nearly perpendicular to a unit vector $n_{0z} = \{0, 0, 1\}$ of the oz axis. As such, the voxels containing candidate points of the tank wall are filtered based on a deviation angle between the normal vector of the voxel and n_{0z}, which is given in Eq. 4. Resulted filtering irrelevant voxels is shown in Fig. 3.

$$\mathbf{V}_c = (v_i \in \mathbf{V}, i = [1, N_c] \mid \angle n_i, n_{oz} \geq \alpha_{th}) \tag{4}$$

where α_{th} is the angle threshold, which is set 45 degrees. This threshold is selected based on an observation that if the voxels containing the points of both the tank wall and a floor/ground or a roof, the deviation angle may be approximately 45 degrees.

Next, Step 3 is to estimate a cylinder's parameters representing to the tank wall based on the normal vector and center of the voxels $\mathbf{V}_c$. The cylinder can describe by the cylinder's direction $t_c = \{t_x, t_y, t_z\}$, a point $c_c = \{x_c, y_c, z_c\}$ along the t_c, a radius (r_c). In theory, if there are three points (p_1, p_2, p_3) and their normal vectors (n_1, n_2, n_3) on the cylinder, the direction t_c is a cross-product of a pair of the normal vectors, for example, $t_c = n_1 x n_2$. Moreover, when projected these points on an orthogonal plane of the t_c, these projected points locate on a circle. As such, the fitting circle through three projected points can give the center c_c and the radius r_c of the cylinder. Thus, the

cylinder's parameters were determined based on voxels as following. First, the subset voxels, $\mathbf{V}_s = (v_i = \{p_{kNN0i}, n_i\}, i = [1, N_s] \mid \mathbf{V}_s \subset \mathbf{V}_c \})$ were randomly extracted from the $\mathbf{V}_c$. The rPCA (Laefer & Truong-Hong, 2017) was employed to estimate the normal vector of the fitting surface through the normal vectors $\mathbf{n}_s$ of the $\mathbf{V}_s$, which is the direction t_c of the cylinder's axis. The voxel v_{si} can be considered as an outlier voxel if the angle between its normal vector n_{si} and the t_c is larger than a predefined angle threshold (α_{nt}), in which the α_{nt} by 85 degrees was empirically adopted. The process is iteratively removed the outlier voxels until the angle of the t_c from two consecutive iterations is less than a predefined angle by 1 degree (Fig. 4a and b).
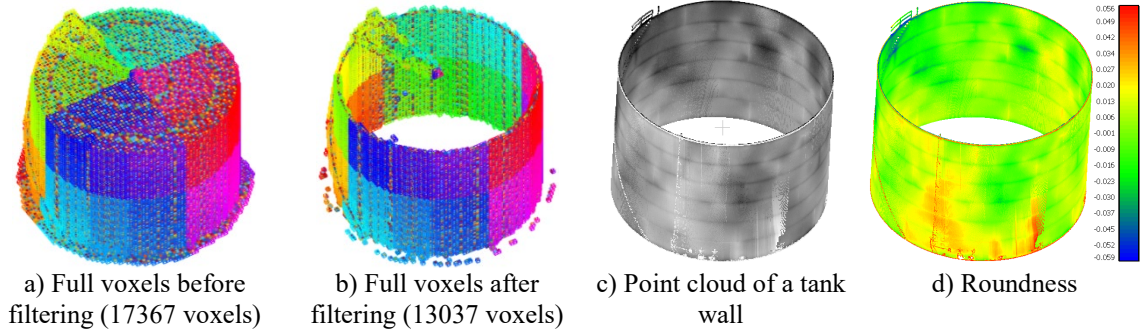

| a) Full voxels before filtering (17367 voxels) | b) Full voxels after filtering (13037 voxels) | c) Point cloud of a tank wall | d) Roundness |

Figure 3. Extracting the voxels possessed candidate points and resulted point clouds of the tank wall

| a) A normal vector space at the first iteration | b) A normal vector space at the last iteration | c) A fitting circle at the first iteration | d) A fitting circle at the last iteration |

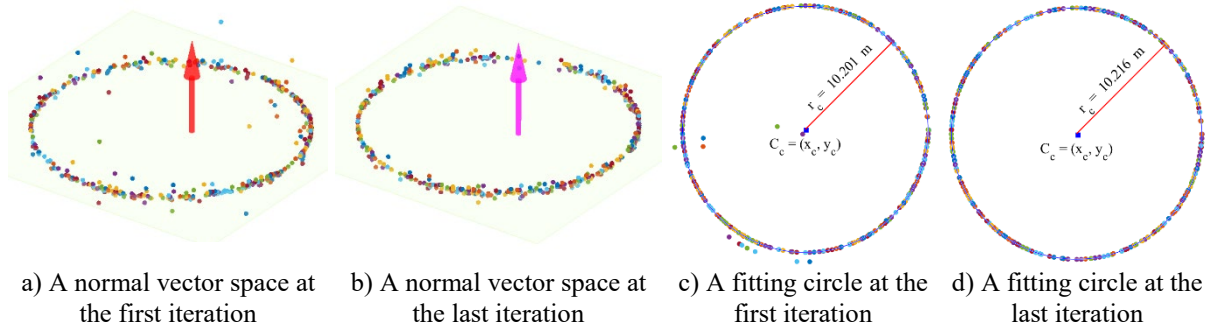**Figure 4**. Interaction process to estimate the direction, centre and radius of the cylinder

Second, the centers of the inlier voxels ($\mathbf{V}_{inlier,s} \subset \mathbf{V}_s$) are projected onto the best fit surface along the t_c. The best fit circle (C_s) through the projected points was iteratively generated by using a least squares method, in which the radius and the centroid of C_s are respectively the radius (r_c) and center $c_c = (x_c, y_c, z_c)$ of the cylinder. Notably, any projected point having the fitting error larger than a maximum distance (ε_{max}) from the points to the detected cylinder is eliminated and the convergence is obtained when no the projected point to be eliminated (Fig. 4 c and d). Finally, the number of the points within the ε_{max} of the fitting cylinder C_{tw} are used as a score to determine the best fit cylinder having the largest number of points, which is given in Eq. 5.

$$\mathbf{P}_{tw} = (p_i \mid p_i \in \mathbf{P} \, \Lambda \, \varepsilon_{pi} \leq \varepsilon_{max}) \tag{5}$$

where $d(p_i, C_{tw})$ is the distance from the point to the $C_{tw}(c_c, r_c, t_c)$, which is expressed in Eq. 6.

$$\varepsilon_{pi} = d(p_i, C_{tw}) = |d(p_i, L_c) - r_c| \tag{6}$$

where $L_c(c_c, t_c)$ is the line through the center of the fitting cylinder C_{tw} with the direction axis t_c.

In Step 4, two critical types of the tank's deformations need to report: (i) best fit vertical deformation and roundness. The best fit vertical deformation measures as a distance from the points to the tank wall assumed as the perfectly vertical cylinder (C_{twv}), which can be expressed in Eq.7. The C_{twv} can be defined as a fitting the circle $C(x_c, y_c, z_c, r_c)$ through projection of all points of the tank wall on a horizontal plane for example the xy plane. Moreover, the roundness is defined that the distance from the point to the tank wall assumed as a perfect cylinder (C_{tw}), which is computed based Eq. 6. Notably, the fitting cylinder here can be an inclined cylinder. Fig. 3d illustrates the roundness.
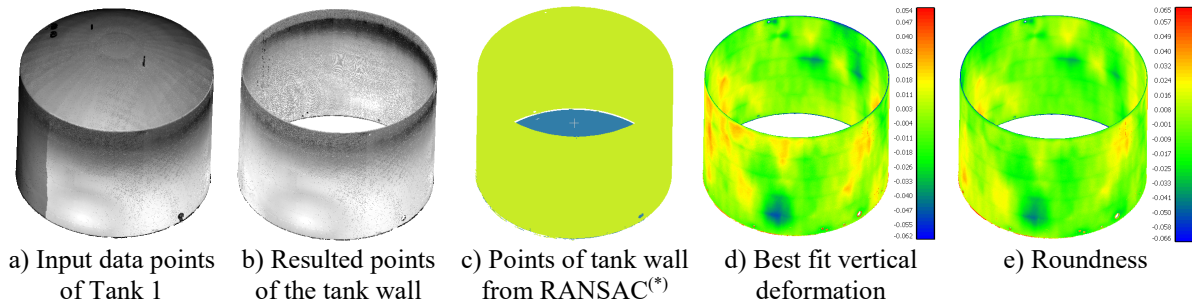
$$\varepsilon_{best\_fit\_vert\_def} = d(p_i, C_{twv}) = |d(p_i, C) - r_c| \tag{7}$$

4   Experimental tests

An aim of the experiment is to evaluate the proposed method in extracting and assessing of the tank wall from a

massive point cloud acquired from a terrestrial laser scanner. Two tanks are selected to test performance of the proposed methods, and results of the tank wall extraction also compare to ones from RANSAC method proposed by Schnabel et al. (2007) plugged in CloudCompare V2.7.0 (CloudCompare). Tank 1 is Tank 67 with a diameter of 18.288m and height of 12.50m, located at Regina, Canada while Tank 2 is Tank 2490 with a diameter of 21.336m and height of 14.63m, located at Houston, US. Both Tanks were captured by Faro Focus X130 with the sampling step by 6.136mm at a measurement range by 10m. After registering the point clouds from different scanning stations, the point clouds are down-sampled with a minimum distance between two adjacent points no more 5mm. The data sets with x-, y-, and z-coordinates are respectively 33,692,139 points and 22,447,931 points for the Tank 1 and 2 as input data. The proposed method is implemented in Matlab programming language and the tests are processed on Dell Precision Workstation with a main system configuration: Intel(R) Xeon(R) W-2123 CPU @ 3.6GHz with 32GB RAM.

Input parameters consisting of the voxel size, $v_{size} = 0.5$m, kNN $= 25$ points, $\alpha_{th} = 45$ degrees, $\alpha_{nt} = 85$ degrees, and $\varepsilon_{max} = 0.05$m are used for both Tanks. Moreover, input parameters for the RANSAC method proposed by Schnabel et al. (2007) are the *min_ptc* $= 10\%$ of size of an input data, the $\varepsilon_{max} = 0.05$m, and $\alpha = 10$ degrees. Resulted extraction of data points and deformation of both Tanks are showed in Fig. 5 and 6. A visualization evaluation is showed that the proposed method can extract proper point clouds of the tanks and is comparable with the Schnabel 's method. The difference of a tank's diameter from the inventory and ones from the proposed method are respectively 0.026m for Tank 1 (18.288m vs. 18.262m) and 0.008m for Tank 2 (21.336m vs. 21.344m). Notably, errors here include errors from a damage of the tank wall, data acquisition and registration and the proposed method.

a) Input data points   b) Resulted points   c) Points of tank wall   d) Best fit vertical   e) Roundness
    of Tank 1   of the tank wall   from RANSAC$^{(*)}$ deformation

$^{(*)}$ *Two cylinders were extracted from the point cloud by the RANSAC method (Schnabel et al. ,2007)*

Figure 5. Resulted extraction of a point cloud of Tank 1 from the proposed method and RANSAC proposed Schnabel et al. (2007) and deformation of the tank from the proposed method

a) Input data points   b) Resulted points   c) Points of tank   d) Best fit   e) Roundness
    of Tank 2   of the tank wall   wall from RANSAC   vertical deformation

Figure 6. Resulted extraction of a point cloud of Tank 2 from the proposed method and RANSAC proposed Schnabel et al. (2007) and deformation of the tank from the proposed method
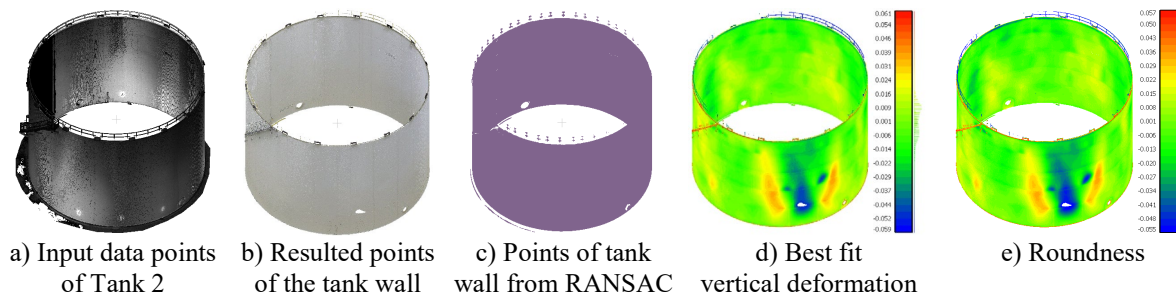
As the tank wall is assumed as a perfect cylinder when implementing the method to extract the tank wall point cloud, resulted point clouds of adjacent objects of the tank wall are also included, for example, the points of safeguard and ground (Fig. 5b and c, and Fig. 6b and c). This issue can be solved when an additional localized filtering is implemented. Moreover, the proposed method may be under-extraction of the tank wall's points when the wall is subjected to deformation larger than the than a maximum distance (ε_{max}).

The executing time from the proposed method are 697.5s for Tank 1 and 504.4s for Tank 2. Comparatively, ones from the RANSAC method proposed by Schnabel et al. (2007) are respectively 514.8s and 335.0s. However, it is noticed that the RANSAC method was implemented in C++ programming language. Moreover, in the proposed method, only the maximum distance ε_{max} affects to the results while in the RANSAC method (Schnabel et al., 2007) 3 input parameters (*min_ptc, ε_{max}, α*) are required to obtain the best result. Finally, by using the

RANSAC method (Schnabel et al., 2007) for this application, multiple cylinders can be obtained, and additional filtering is needed to determine the correct cylinder of the tank wall, for example, there are 2 cylinders extracted for Tank 1 (Fig. 5c).

5   Conclusions

This paper presents a new, efficient RANSAC-based voxelization method to extract a cylinder representing to a wall of a storage tank from a massive data point cloud. The input data points are decomposed by an octree representation and the voxels containing candidate points of the tank wall are extracted by examining normal vectors of the voxels, which are computed from the kNN points of the voxel center. Next the RANSAC paradigm is applied on a subset voxel to estimate the direction axis, center, radius of the cylinder. In this step, an outlier removal process is applied to eliminate the outlier voxels. The proposed method is tested on two Tanks scanned from outside and inside of the tanks. The experimental tests show the points of the tank walls are successfully extracted and comparable with the popular RANSAC method. The results also show that diameters of the extracted cylinders differ from ones derived from an inventory about 0.026m (Tank 1) and 0.008m (Tank 2). Moreover, the executing time is respectively 697.5s and 504.4s for the data set of 33,692,139 points and 22,447,931 points. However, the point cloud of the tank wall still contains data points of other objects closed to the tank wall, which can be removed by implementing a local outlier filter. Finally, as the tank is often subjected to deformation, selecting an appropriate maximum distance is still difficulty.

Acknowledgements

References

Bosché, F., Ahmed, M., Turkan, Y., Haas, C. T., & Haas, R. (2015). The value of integrating Scan-to-BIM and Scan-vs-BIM techniques for construction monitoring using laser scanning and BIM: The case of cylindrical MEP components. *Automation in Construction, 49*, 201-213. doi:https://doi.org/10.1016/j.autcon.2014.05.014

CloudCompare (Version 2.7.0). Retrieved from http://www.cloudcompare.org/

Figueiredo, R., Dehban, A., Moreno, P., Bernardino, A., Santos-Victor, J., & Araújo, H. (2019). A robust and efficient framework for fast cylinder detection. *Robotics and Autonomous Systems, 117*, 17-28. doi:https://doi.org/10.1016/j.robot.2019.04.002

Laefer, D. F., & Truong-Hong, L. (2017). Toward automatic generation of 3D steel structures for building information modelling. *Automation in Construction, 74*, 66-77. doi:https://doi.org/10.1016/j.autcon.2016.11.011

Laefer, D. F., Truong-Hong, L., Carr, H., & Singh, M. (2014). Crack detection limits in unit based masonry with terrestrial laser scanning. *NDT & E International, 62*, 66-76. doi:http://dx.doi.org/10.1016/j.ndteint.2013.11.001

Maalek, R., Lichti, D. D., Walker, R., Bhavnani, A., & Ruwanpura, J. Y. (2019). Extraction of pipes and flanges from point clouds for automated verification of pre-fabricated modules in oil and gas refinery projects. *Automation in Construction, 103*, 150-167. doi:https://doi.org/10.1016/j.autcon.2019.03.013

Nurunnabi, A., Sadahiro, Y., Lindenbergh, R., & Belton, D. (2019). Robust cylinder fitting in laser scanning point cloud data. *Measurement, 138*, 632-651. doi:https://doi.org/10.1016/j.measurement.2019.01.095

Rabbani, T., & Van Den Heuvel, F. (2005). Efficient hough transform for automatic detection of cylinders in point clouds. *ISPRS WG III/3, III/4, 3*, 60-65.

Schnabel, R., Wahl, R., & Klein, R. (2007). Efficient RANSAC for point-cloud shape detection. *Computer Graphics Forum*, 26(2), 214-226

Tran, T.-T., Cao, V.-T., & Laurendeau, D. (2015). Extraction of cylinders and estimation of their parameters from point clouds. *Computers & Graphics*, 46, 345-357. doi:https://doi.org/10.1016/j.cag.2014.09.027

Truong-Hong, L., & Laefer, D. (2015). Documentation of Bridges by Terrestrial Laser Scanner. *the IABSE Geneva Conference 2015*, Geneva, Switzerland, 22-25 Sep., 2015

Truong-Hong, L., & Laefer, D. F. (2014). Octree-based, automatic building façade generation from LiDAR data. *Computer-Aided Design*, 53, 46-61. doi:https://doi.org/10.1016/j.cad.2014.03.001

Truong-Hong, L., Laefer, D. F., Hinks, T., & Carr, H. (2012). Combining an angle criterion with voxelization and the flying voxel method in reconstructing building models from LiDAR data. *Computer-Aided Civil and Infrastructure Engineering*, 28(2), 112-129.